

# Thermal stability of microscale additively manufactured copper using pulsed electrodeposition

Soheil Daryadel <sup>a</sup>, Majid Minary-Jolandan <sup>b,\*</sup>

<sup>a</sup> Department of Materials Science and Engineering, University of Illinois at Urbana-Champaign, Urbana, IL 61801, USA

<sup>b</sup> Department of Mechanical Engineering, The University of Texas at Dallas, Richardson, TX 75080, USA



## ARTICLE INFO

### Article history:

Received 27 May 2020

Received in revised form 4 August 2020

Accepted 23 August 2020

Available online 27 August 2020

### Keywords:

Microscale additive manufacturing (AM) of metals

Localized electrodeposition

Microscale 3D printing

Interconnects

Thermal stability

## ABSTRACT

Micro/nanoscale 3D printing of metals is promising for printed electronics and sensors. It is important to evaluate how material properties of the microscale 3D-printed metals change at high temperature, though such studies are currently very limited. Here, we investigate morphological and mechanical property changes in copper interconnects 3D-printed by pulsed electrodeposition process. The results revealed significant surface damage and void formation in printed Cu after annealing at 450 °C. No significant surface damages or voids were observed for printed Cu annealed at 300 °C, however, their strength dropped ~40% from the strength of the as-deposited material (~868 MPa). Such results are important to determine the operation temperature range for interconnects fabricated by microscale 3D printing.

© 2020 Elsevier B.V. All rights reserved.

## 1. Introduction

The recent progress in 3D printing of metals and alloys at microscale promises an emerging area for printed electronics and sensors [1–6]. The meniscus confined electrodeposition is a microscale 3D printing process with the advantage that pure crystalline metals and alloys can be deposited electrochemically without any polymer additives [2–10]. Using electrodeposition, nanocrystalline (nc) and nanotwinned (nt) metals can be obtained by application of direct current and pulsed current, respectively [11]. Microstructure evolution of metals at elevated temperature, which usually causes unexpected failure in systems, is a major challenge in critical applications in which any changes in materials properties will affect system performance. Hence, it is important to evaluate how material properties of the microscale 3D-printed metals change at high temperature, in particular temperature that they may be exposed to in electronics and sensors. In this article, we investigate the thermal stability of copper (Cu) printed using the localized pulsed electrodeposition process (Fig. 1A). In this process, metal is 3D-printed using pulsed electrodeposition at the tip of an electrolyte-containing nozzle [7,12]. The goal is to determine the operation temperature range for interconnects fabricated using this additive manufacturing process.

## 2. Materials and methods

### 2.1. The printing process

Copper (Cu) micro-pillars were printed using a glass micropipette nozzle with a diameter of ~5 µm. The micropipette was filled with an electrolyte of CuSO<sub>4</sub> (100 mM) and H<sub>2</sub>SO<sub>4</sub> (1 M). A copper wire was used as the anode, and a gold-coated silicon substrate served as the cathode electrode. Pulsed current was applied between the two electrodes using a potentiostat to deposit Cu. A high resolution nano-positioning system was employed to control the substrate motion. The synchronized motion of the substrate and simultaneous metal deposition results in 3D printing of Cu micro-pillars. During deposition a pulsed voltage with an on-time of 0.02 s, an off-time of 1.98 s, and a peak current density of 7.27 A/cm<sup>2</sup> was used.

### 2.2. Thermal annealing

The samples were annealed separately at 150 °C, 300 °C, and 450 °C for 4-hour using the infrared lamp heater in a sputtering chamber maintained at a vacuum pressure of ~5 × 10<sup>-6</sup> Pa. The heating rate was 10 °C/min, and the samples were cooled down to room temperature after heat treatment at the average rate of ~3 °C/min. Argon gas flow was used to increase the cooling rate.

\* Corresponding author.

E-mail address: [majid.minary@utdallas.edu](mailto:majid.minary@utdallas.edu) (M. Minary-Jolandan).

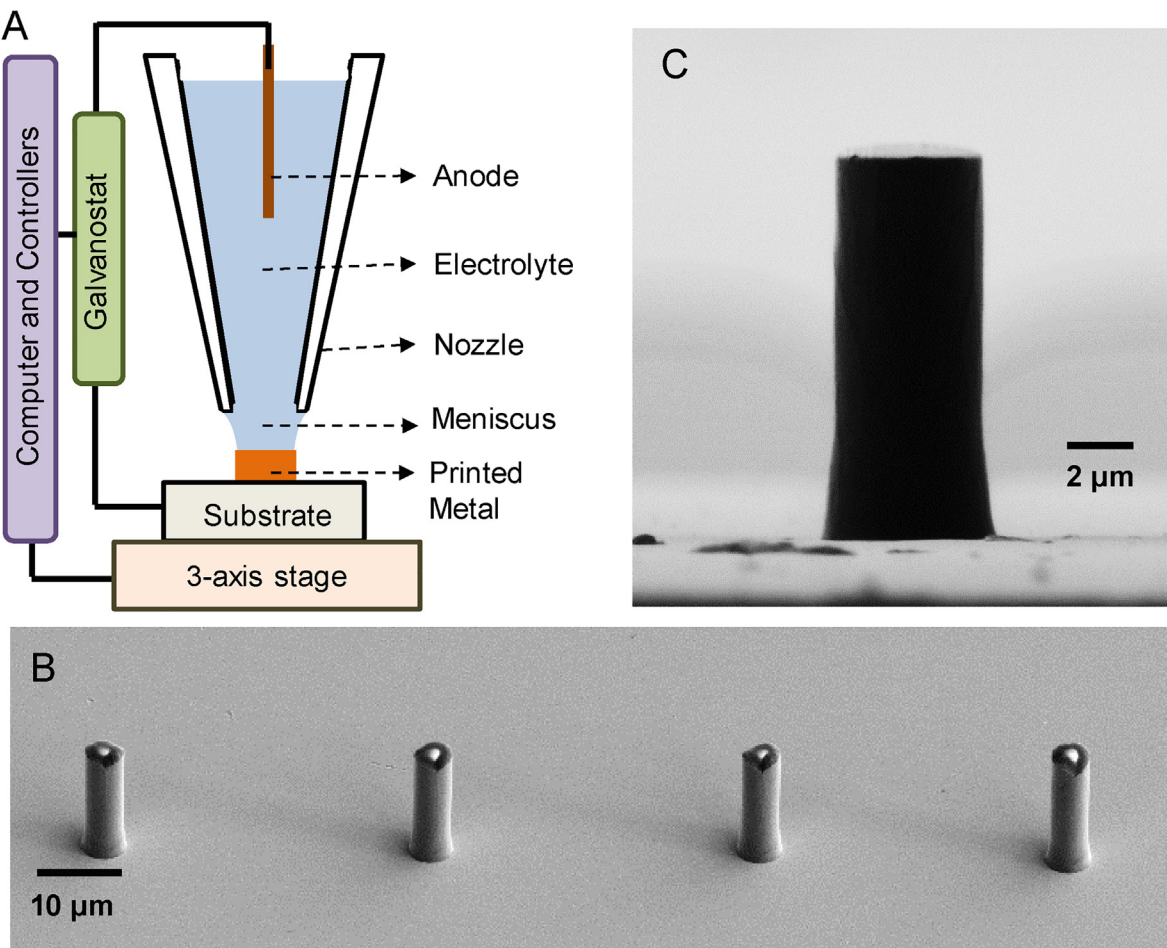


**Fig. 1.** (A) The schematic view of the microscale electrochemical 3D-printing process. (B) An array of printed micro-pillars. (C) A close-up view of a 3D-printed micro-pillar.

### 2.3. Microstructure characterization

The microstructure of the 3D-printed Cu was characterized utilizing scanning electron microscopy (SEM, Zeiss Supra 40) and high-resolution focused ion beam (FIB, FEI Nova Nanolab 200).

### 2.4. Mechanical characterization

*In situ* micro-compression experiments were carried out using an *in-situ* SEM nanoindentation system (NanoFlip, Nanomechanics) with a 50 μm diameter conductive diamond flat punch. Three samples were tested for each condition. The average diameter of the samples was  $\sim 4.5 \pm 0.1 \mu\text{m}$  with the length-to-diameter ratio of  $\sim 2.7:1$  to minimize the buckling effects.

## 3. Results

Fig. 2B, C demonstrates the feasibility of direct printing of an array of Cu micro-pillar/bumps using the pulsed electrodeposition process. To investigate the thermal stability of 3D-printed Cu, micro-pillars were directly printed, and subsequently annealed at three different temperatures (150 °C, 300 °C, and 450 °C) for 4 h.

The post-annealed surface morphology of pillars was investigated for different annealing temperatures. The surfaces of the μ-pillars were relatively smooth and undamaged for pillars annealed at 150 °C and 300 °C (Fig. 2A-C). We note that the micro-pillar in Fig. 2C shows different surface morphology compared to the as-

deposited and annealed at 150 °C micro-pillar, in particular at the bottom and at the top surface. We believe that the bottom part is the effect of the “seed layer”. This layer serves as nuclei at the substrate interface, and plays a critical role in the microstructure of the samples. There exists an ultrafine grained transition layer between the seed layer and the preferred (111) orientation nt-Cu. We believe that the bottom layer difference between the pillars primarily arises from the damage to this region, as it is more pronounced for the pillar in Fig. 2D. The top section of the pillars in Fig. 2C and D are also different than the ones in Fig. 2A and B, which shows the effect of more damage caused at the top section.

The FIB (focused ion beam) was utilized to observe the microstructure evolution in pillars' cross-section after heat treatment (Fig. 2E-H). Fig. 2E shows the nanotwinned (nt) microstructure of the as-deposited pillar with an average grain size of  $\sim 420 \text{ nm}$ . The detailed microstructural analysis of the printed nt microstructures using L-PED process have been presented in the authors' recent publications.[12,13] The microstructure remained relatively stable for pillars annealed at 150 °C. At 300 °C, the grains grew larger (average grain size of 490 nm), however, the TBs were still stable (Fig. 2G). For the pillar annealed at 450 °C, large grains (average grain size of 860 nm) and voids were observed.

The compression strength of the micro-pillars was examined *in situ* SEM using micro-compression (Fig. 3A-C). Fig. 3D shows representative true stress-strain responses from these experiments. Fig. 3E shows the comparison of the flow stress for the pillars. An elastic-plastic behavior was observed with rather large ductility (Fig. 3D). It is evident that the strength decreased after

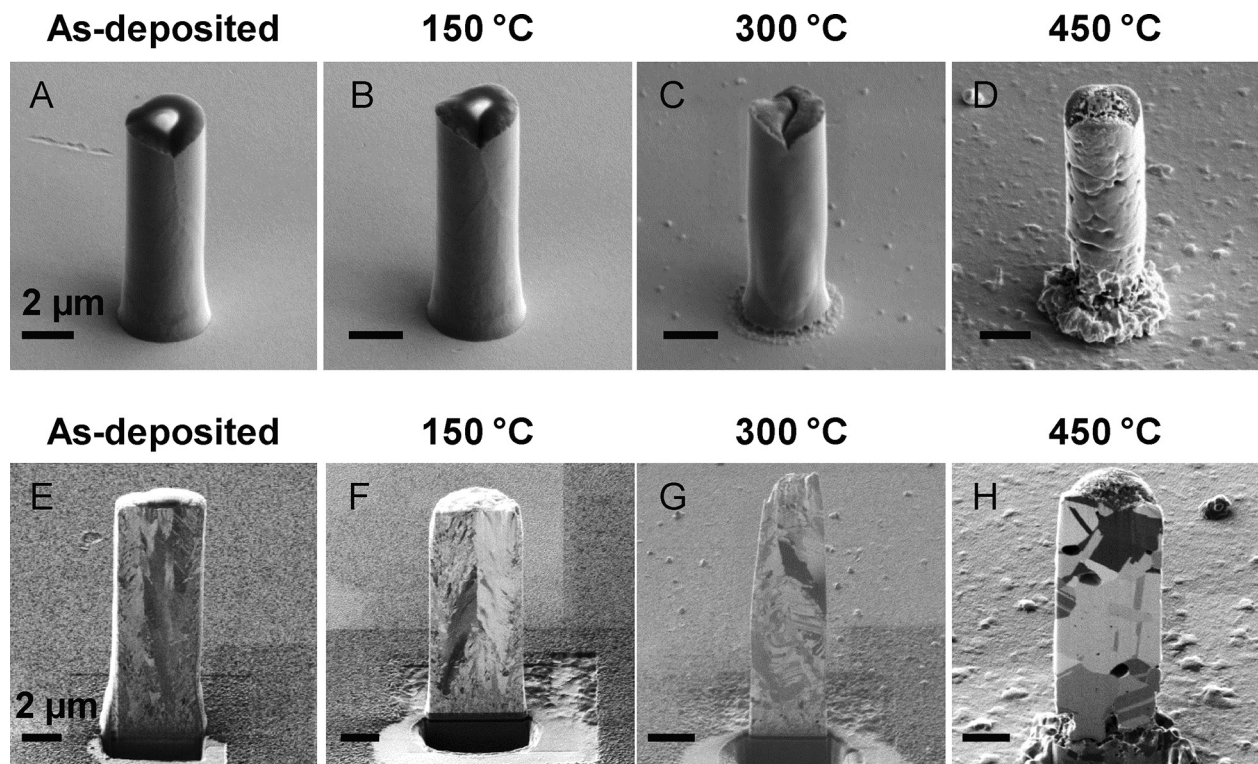


**Fig. 2.** SEM images of Cu micro-pillars (A) as-deposited, and after 4-hour annealing at (B) 150 °C (C), 300 °C, and (D) 450 °C. All scale bars are 2  $\mu$ m. The cross-section FIB ion contrast images show the microstructure of Cu micro-pillars: (E) as-deposited and after 4-hour annealing at (F) 150 °C (G) 300 °C (H) 450 °C. All scale bars are 2  $\mu$ m.

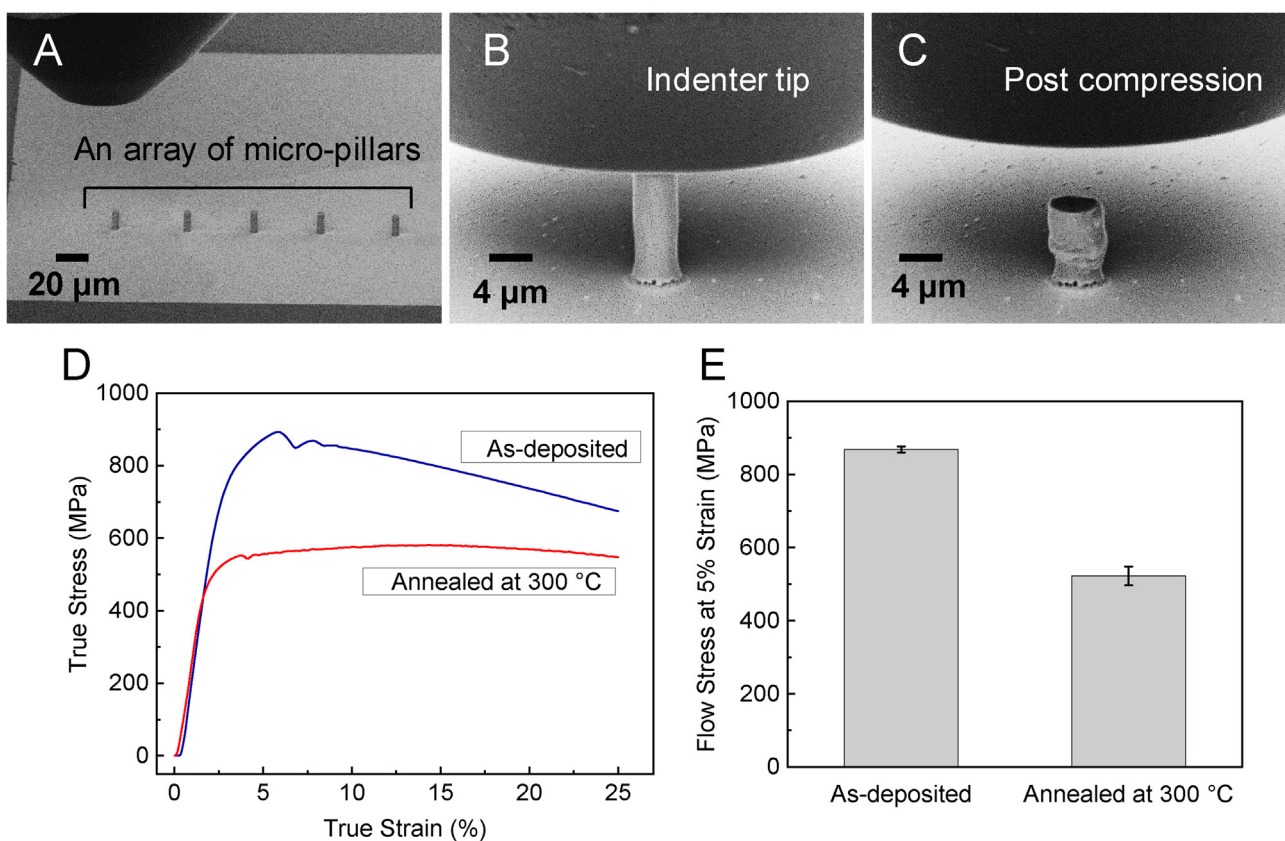


**Fig. 3.** (A) *In situ* SEM micro-compression experiment on an array of 3D printed Cu micro-pillars. (B) The close-up SEM view of a micro-pillar at the beginning of the test. (C) An SEM image of compressed micro-pillar. (D) The true stress-strain responses of the printed micro-pillars for as-deposited condition, and after annealing for 4-hour at 300 °C. (E) The comparison of the average flow stress.

annealing. The flow stress of printed Cu decreased to approximately  $522 \pm 25$  MPa after 4-hour annealing at  $300^\circ\text{C}$ , a ~40% reduction.

We note that the same parameters (pulsed voltage and the electrolyte) were used to print the pillars. In addition to these imposed processing parameters, there are instabilities associated with the moving "meniscus" between the nozzle tip and the growth front of the pillar. These liquid instabilities can cause small fluctuations in the printed diameter between different pillars, and this in turn can cause slight variation in the apparent diameter, and top surface of the pillar, when the nozzle separates from the pillar at the end of the process. We have used samples with flat top surface for mechanical characterization.

#### 4. Discussion

The printed pillars are stable over time. The presented SEM images were taken weeks after deposition. In Cu the energy stored in high-angle GBs (grain boundaries) is approximately 20-time higher than the twin boundary (TB) energy [14]. Therefore, the driving force for grain growth is more than the force required for coarsening TBs thickness [15]. The thermal stability of nt-Cu is attributed to close-packed atomic arrangement of coherent TBs and their low energy compared to the grain boundaries (GBs), which makes coherent TBs less mobile at a higher temperature. Once the temperature exceeds a critical temperature range, grains started growing abnormally and coalesced. The flow stress of the as-deposited pillars ranged from 860 MPa to 875 MPa with an average of  $868 \pm 8$  MPa, which is remarkable for 3D printed Cu. In Cu deposited by pulsed electrodeposition, the twin boundaries block the motion of intersecting dislocations, which increases the strength of the material.

The drop of strength after annealing is attributed to larger grains and increased twin thickness after annealing. The results show that despite the significant drop in the strength of printed structure after annealing, considering the superior mechanical and electrical properties of nt-Cu compared to coarse-grained and nanocrystalline Cu, the L-PED process can be reliably used for temperatures as high of  $300^\circ\text{C}$ . The formation of voids is not desirable in Cu interconnects because it increases the electrical resistance and reduces mechanical strength.

In this manuscript, we aimed to evaluate how material properties of the microscale 3D-printed copper changed in extreme conditions, especially the high temperature that they may be exposed to in electronic applications. Pillars annealed at  $450^\circ\text{C}$  were not considered for the mechanical testing due to extensive surface damages consisting of the grooves and voids. Considering the change of microstructure and post-annealing surface morphology at  $300^\circ\text{C}$ , we were interested in looking at the mechanical properties of the annealed pillars. Indeed, full characterization for a wider temperature range is being considered for our future work.

We have previously reported the comparison of the mechanical properties of nanotwinned copper micro-pillars and other reported nanotwinned materials in the form of electrodeposited or sputtered bulk solids and films, or nanopillars fabricated using FIB milling or template patterning in Ref. [16]. The results show that L-PED has the capability of fabricating pristine controlled microstructure with comparable mechanical properties to the bulk sample.

During heat treatment, the material is subjected to thermal strain. Since the local elastic modulus can be different for grains with different orientation, this anisotropy in grains may result in different thermal stresses, which would cause stress concentration at the interfaces to satisfy the boundary conditions [17]. During the annealing process, the density of strong texture is decreased, the

diffusion is enhanced, and therefore, voids are formed at a GB triple junction. The energy for nucleation of a void is estimated to be twice the surface energy minus the twin interface energy [17,18]. The small twin interface energy in coherent twins renders the void formation in the presence of concentrated stress more difficult. At regions with stress concentration, the voids are formed by interface decohesion failure and become rounded in shape by diffusion.

#### 5. Conclusions

This work was motivated by recent advances in microscale additive manufacturing of metals that makes it possible to directly print interconnects and micro-bumps. For realization of this process and application of the printed metal in electronics and sensors, it is desirable to find the maximum operation temperature. The results revealed significant surface damage and void formation in the Cu pillars after annealing for 4 h at  $450^\circ\text{C}$ . No significant surface damages or voids were observed for the pillars annealed at  $300^\circ\text{C}$ , however, their strength dropped ~40% from the strength of the as-deposited material (~868 MPa). The exact operation temperature window for printed nt-Cu will ultimately depend on each particular application. Future work should focus on engineering the microstructure (grain size and twin density) using process parameters to fine-tune or enhance the stable temperature range. Such progress combined with remarkable properties of nt-Cu will accelerate the application of 3D printed nt-Cu in the electronics industry.

#### Author contributions

Both authors designed the work. SD performed the experiments. SD and MMJ wrote the article.

#### Declaration of Competing Interest

The authors declare that they have no known competing financial interests or personal relationships that could have appeared to influence the work reported in this paper.

#### Acknowledgment

This work was supported by the NSF-CMMI (award # 1727539).

#### References

- [1] L. Hirt et al., Additive manufacturing of metal structures at the micrometer scale, *Adv. Mater.* 29 (17) (2017) 1604211.
- [2] J. Hu, M.-F. Yu, Meniscus-confined three-dimensional electrodeposition for direct writing of wire bonds, *Science* 329 (5989) (2010) 313.
- [3] S. Daryadel et al., Localized pulsed electrodeposition process for three-dimensional printing of nanotwinned metallic nanostructures, *Nano Lett.* 18 (1) (2017) 208–214.
- [4] L. Hirt et al., Template-free 3D microprinting of metals using a force-controlled nanopipette for layer-by-layer electrodeposition, *Adv. Mater.* 28 (12) (2016) 2311–2315.
- [5] Y. Lei et al., Dynamic "scanning-mode" meniscus confined electrodepositing and micropatterning of individually addressable ultraconductive copper line arrays, *J. Phys. Chem. Lett.* 9 (9) (2018) 2380–2387.
- [6] Q. Huang, R. Gyorgak, R. Pak, Electrochemical formation of free-standing 3D structures using injection of additives, *J. Electrochem. Soc.* 164 (12) (2017) D737–D743.
- [7] A. Behroozfar et al., Additive printing of pure nanocrystalline nickel thin films using room environment electroplating, *Nanotechnology* 31 (5) (2019) 055301.
- [8] C. Wang et al., Direct-write printing copper-nickel (Cu/Ni) alloy with controlled composition from a single electrolyte using co-electrodeposition, *ACS Appl. Mater. Interfaces* 12 (16) (2020) 18683–18691.
- [9] A.P. Suryavanshi, M.-F. Yu, Probe-based electrochemical fabrication of freestanding Cu nanowire array, *Appl. Phys. Lett.* 88 (8) (2006) 083103.
- [10] Y.-P. Lin, Y. Zhang, M.-F. Yu, Parallel process 3D metal microprinting, *Adv. Mater. Tech.* 4 (1) (2019) 1800393.

- [11] A. Behroozfar et al., Microscale 3D printing of nanotwinned copper, *Adv. Mater.* 30 (4) (2018) 1705107.
- [12] S. Daryadel et al., Localized pulsed electrodeposition process for three-dimensional printing of nanotwinned metallic nanostructures, *Nano Lett.* 18 (1) (2018) 208–214.
- [13] S. Daryadel, A. Behroozfar, M. Minary-Jolandan, Toward control of microstructure in microscale additive manufacturing of copper using localized electrodeposition, *Adv. Eng. Mater.* 21 (1) (2019) 1800946.
- [14] X. Zhang, A. Misra, Superior thermal stability of coherent twin boundaries in nanotwinned metals, *Scr. Mater.* 66 (11) (2012) 860–865.
- [15] Y. Zhao et al., Thermal stability of highly nanotwinned copper: The role of grain boundaries and texture, *J. Mater. Res.* 27 (24) (2012) 3049–3057.
- [16] S. Daryadel, A. Behroozfar, M. Minary-Jolandan, A microscale additive manufacturing approach for *in situ* nanomechanics, *Mater. Sci. Eng., A* 767 (2019) 138441.
- [17] J. Koike et al., A relationship between film texture and stress-voiding tendency in Copper thin films, *AIP Conf. Proc.* 612 (1) (2002) 169–176.
- [18] A. Sekiguchi, J. Koike, K. Maruyama, Microstructural influences on stress migration in electroplated Cu metallization, *Appl. Phys. Lett.* 83 (10) (2003) 1962–1964.